

Phosphorylation of SOCS1 Inhibits the SOCS1-p53 Tumor Suppressor Axis

Emmanuelle Saint-Germain¹, Lian Mignacca¹, Geneviève Huot¹, Mariana Acevedo¹, Karine Moineau-Vallée¹, Viviane Calabrese¹, Véronique Bourdeau¹, Marie-Camille Rowell^{1,2}, Subburaj Ilangumaran³, Frédéric Lessard¹, and Gerardo Ferbeyre^{1,2}



Abstract

Expression of the suppressor of cytokine signaling-1 (SOCS1) is inactivated in hematopoietic and solid cancers by promoter methylation, miRNA-mediated silencing, and mutations. Paradoxically, SOCS1 is also overexpressed in many human cancers. We report here that the ability of SOCS1 to interact with p53 and regulate cellular senescence depends on a structural motif that includes tyrosine (Y)80 in the SH2 domain of SOCS1. Mutations in this motif are found at low frequency in some human cancers, and substitution of Y80 by a phosphomimetic residue inhibits p53-SOCS1 interaction and its functional consequences, including stimulation of p53 transcriptional activity, growth arrest, and cellular senescence. Mass spectrometry confirmed SOCS1 Y80 phosphorylation in cells, and a new mAb was generated to detect its presence in tissues by IHC. A tyrosine kinase library screen identified the

SRC family as Y80-SOCS1 kinases. SRC family kinase inhibitors potentiated the SOCS1-p53 pathway and reinforced SOCS1-induced senescence. Samples from human lymphomas that often overexpress SOCS1 also displayed SRC family kinase activation, constitutive phosphorylation of SOCS1 on Y80, and SOCS1 cytoplasmic localization. Collectively, these results reveal a mechanism that inactivates the SOCS1-p53 senescence pathway and suggest that inhibition of SRC family kinases as personalized treatment in patients with lymphomas may be successful.

Significance: These findings show that SOCS1 phosphorylation by the SRC family inhibits its tumor-suppressive activity, indicating that patients with increased SOCS1 phosphorylation may benefit from SRC family kinase inhibitors.

Introduction

SOCS1 is a 211-amino acid protein composed of a central SH2 (src homology) domain and a C-terminal domain called the SOCS box (1). The SH2 domain of SOCS1 recognizes target proteins that are ubiquitinated and targeted to the proteasome by the E3 ligase complex bound to the SOCS box (2). SOCS1 also binds to the tumor suppressor p53 but does not stimulate its degradation (3–5). The SH2 domain of SOCS1 interacts with the N-terminal transactivation domain of p53, while the C-terminal domain of SOCS1, containing the SOCS Box, mediates interaction with the DNA damage-regulated kinases ATM/ATR. SOCS1 thus serves as an adaptor

for ATM/ATR-dependent phosphorylation of p53 and the activation of its tumor-suppressive functions (3, 5–7).

SOCS1 expression is reduced in human cancers due to DNA methylation or miRNA-mediated silencing (4, 8–15). In addition, in some patients with primary mediastinal B-cell lymphoma (16), diffuse large B-cell lymphoma (DLBCL; ref. 17) and many patients (61%) with Hodgkin lymphoma, SOCS1 is mutated (18, 19). In addition, enforced expression of SOCS1 in many different tumor cell types leads to a potent antiproliferative activity (3, 20). Taken together, the data referred above denote that SOCS1 is a tumor suppressor gene. On the other hand, SOCS1 can also exert oncogenic activities, as shown by its increased levels in colorectal cancer, melanoma, and in a mouse model of FTL3-induced myeloproliferative disease (21–23). The molecular mechanisms explaining how SOCS1 displays contrasting activities in tumors remain to be identified.

One hallmark of tumor cells is their ability to sustain cell proliferation, typically by activating tyrosine kinase signaling pathways (24). Tyrosine kinases altered in cancers include receptor tyrosine kinases that initiate signal transduction pathways via both serine/threonine kinases and non-receptor tyrosine kinases (25). These kinases may phosphorylate and inhibit the function of tumor suppressors (26). Here we report that SOCS1 interacts with p53 using a novel protein-protein interaction motif that comprises amino acids F79, Y80, and W81 of SOCS1. Phosphorylation of Y80 in this motif was confirmed by mass spectrometry and kinase assays and was found to be carried out by the SRC family of non-receptor

¹Département de Biochimie et Médecine Moléculaire, Université de Montréal, Montréal, Québec, Canada. ²CRCHUM, Montréal, Québec, Canada. ³Department of Anatomy and Cell Biology, Faculty of Medicine, University of Sherbrooke, Sherbrooke, Canada.

Note: Supplementary data for this article are available at Cancer Research Online (<http://cancerres.aacrjournals.org/>).

Corresponding Authors: Gerardo Ferbeyre, University of Montréal, 2900 Edouard Montpetit, Roger Gaudry E515, Montréal, Québec H3C3J7, Canada. Phone: 514-343-7571; Fax: 514-343-2210; E-mail: g.ferbeyre@umontreal.ca; Frédéric Lessard, frederic.lessard@umontreal.ca

Cancer Res 2019;79:3306–19

doi: 10.1158/0008-5472.CAN-18-1503

©2019 American Association for Cancer Research.

tyrosine kinases. Importantly, Y80 phosphorylation interfered with p53 binding and induction of senescence but treatment with SRC-family tyrosine kinase inhibitors restored p53 binding and potentiated the senescence response to SOCS1 expression. Development of a phospho-specific mAb against phosphorylated SOCS1 (Y80) allowed us to observe by IHC an increase in SOCS1 phosphorylation at Y80 in human lymphomas in correlation with increased activation of SRC family kinases and a cytosolic localization of SOCS1.

Materials and Methods

Cell lines, reagents, and retroviral gene transfer

See Table 1 for cell lines used and culture conditions.

Adherent cells were trypsinized using 0.25X Trypsin-EDTA (Life Technologies, catalog no. 15090-046). Doxorubicin (Sigma) was used at a concentration of 300 ng/mL. Serum starvation experiments were performed by culturing the cells in medium without serum for 16 hours before treating with 100 ng/mL EGF (Life Technologies). Dasatinib (#S1021) and saracatinib (#S1006) were purchased from Selleckchem and resuspended in DMSO and ethanol, respectively. Cells were treated with the selected compounds at doses ranging from 1 nmol/L to 80 nmol/L for long-term treatments, the drug being changed every two days. For signaling experiments, cells were treated with 100 nmol/L dasatinib for 2 hours prior to cell collection. IFN β was a kind gift of Biogen and was used at a final concentration of 1,000 U/mL.

Retroviral-mediated gene transfer was performed as described previously (28). Infected cell populations were selected with either puromycin (2.5 μ g/mL, 3 days) or hygromycin (80 μ g/mL, 5 days). For U2OS cells infected with pWZLneo containing the kinases in combination with pLPC-SOCS1, cells were selected with G418 (600 μ g/mL, 7 days) and puromycin (2 μ g/mL, 3 days). All vectors are described in Supplementary Information.

Colony assays, growth curves, and senescence-associated β -galactosidase staining

For colony assays, U2OS cells were transiently transfected using the calcium phosphate method with 20 μ g of each vector. Cells were selected with 1.5 μ g/mL of puromycin for 3 days, counted, and plated in 6-well plates (10,000 cells per well). Cells were fixed with 1% glutaraldehyde at day 0 to account for plating and at day 10 of growth and then colored with crystal violet. The cell-retained dye was resuspended in 10% acetic acid and quantified using a

Table 2. Protocol

Antibody	Company	Cat #	Dilution	Incubation	Species	Beads
p53	Cell signaling	9282	1:200	O/N 4°C	Rabbit	Sepharose 4B Protein A, Sigma # P9424
p73	Bethyl	A300-126A	1:200	O/N 4°C	Rabbit	
c-YES	Santa Cruz Biotechnology	sc-14	1:200	O/N 4°C	Rabbit	
Cyclin A	Santa Cruz Biotechnology	sc-596	1:200	O/N 4°C	Rabbit	
IgG Unstimulated	NEB		1:200	O/N 4°C	Rabbit	

spectrophotometer. For growth curves, IMR90-infected cells were counted and plated after selection in 12-well plates (10,000 cells per well) and fixed every 2–3 days for the indicated number of days. Cells were fixed, stained, and quantified as described for colony assays. Senescence-associated β -galactosidase staining was done as described in ref. 29.

Coimmunoprecipitation

U2OS cells were collected in cell lysis buffer [20 mmol/L Tris-HCl pH 7.5, 150 mmol/L NaCl, 1 mmol/L EDTA, 1 mmol/L EGTA, 1% Triton X-100, 2.5 mmol/L sodium pyrophosphate, 1 mmol/L β -glycerolphosphate and a cocktail of protease inhibitors (Roche)]. Two milligrams of cell extract from each condition was used for IP and 50 μ g was loaded as input (whole cell lysate). The protocol (Table 2) was used as described previously (3).

For the SOCS1 dimerization experiment, three 10-cm petri dishes of each condition were transfected with 10 μ g 6x-Myc-SOCS1 and 10 μ g of FLAG-SOCS1 or FLAG-SOCS1 Δ BOX using the calcium phosphate method. When the constructs were transfected alone, an empty pLPC vector was used to keep the quantity of transfected DNA constant. Media were changed 24 hours posttransfection and cells were harvested 48 hours posttransfection. Cells were lysed using cell lysis buffer, as described above, and sonicated twice for 30 seconds on ice. FLAG-M2 affinity gel (Sigma-Aldrich #A2220) were blocked for 1 hour at 4°C in cell lysis buffer containing 2.5% BSA, 0.16 μ g/ μ L salmon sperm DNA (Sigma-Aldrich) and 0.16 μ g/ μ L *E. coli* tRNA (Sigma-Aldrich), and then washed twice with cell lysis buffer. FLAG immunoprecipitation was performed using 50 μ L of FLAG-M2 affinity gel for 45 minutes at 4°C. Beads were then washed three times for 10 minutes under agitation at 4°C and resuspended in 2 \times Laemmli buffer. Beads were heated for 10 minutes at 100°C prior to loading on an SDS-PAGE gel for Western blotting.

GST pull-down

BL21 *E. coli* strain harboring each of the p53-GST-fusion vectors were used to produce the recombinant proteins in YTA 2X medium (16 g/L tryptone, 10 g/L yeast extract, 5 g/L NaCl) and induced with 0.4 mmol/L IPTG. The following buffers were used: STE buffer (10 mmol/L Tris-HCl pH 8.0, 1 mmol/L EDTA, 100 mmol/L NaCl) supplemented with DTT (5 mmol/L) and a Protease Inhibitor Cocktail (Roche), NETN buffer (10 mmol/L Tris-HCl pH 8.0, 1 mmol/L EDTA, 100 mmol/L NaCl, 0.5% NP-40). Bacteria were lysed with 1 mg/mL lysozyme and glutathione Sepharose-4B beads (Amersham) were used for the GST pull-down assay. The whole procedure was done as described previously (3). 35 [S] methionine was used to label SOCS1 and the pull-downs were loaded onto an SDS gel for electrophoresis and autoradiography. In one case, radioactive detection was substituted for Western blotting with the FLAG antibody (for SOCS1 construct detection).

Table 1. Cell lines and culture conditions

Cell lines	Origin	Cat #	Culture media	Serum	Antibiotics	2 mmol/L L-Glutamine
SU-DHL4	ATCC	CRL-2957	RPMI1640, Wisent (350-000-CL)	10% FBS, Wisent	1% Penicillin G/Streptomycin (Wisent)	Yes
MEFs	Dr. S. Ilangumaran	(27)	DMEM, Wisent cat #310-015-CL			No
U2OS	ATCC	HTB-96				Yes
IMR90	Coriell Institute	I90-79				No
H1299	ATCC	CRL-5803				Yes
293T	ATCC	CRL-1573		5% FBS (Wisent), 5% NCS (Wisent)		Yes
Phoenix Ampho	Dr. S. Lowe					Yes

Saint-Germain et al.

Tissue microarrays

IHC against pSOCS1Y80 and pSRCY416 was performed on a lymphoma human tissue microarray purchased from US Biomax (#LY2086a). This tissue microarray contains 208 samples, 192 lymphomas, and 16 normal lymph nodes. Two independent scorers quantified and scored the staining. Each scorer made three separate counts of 100 cells for every tumor and for every type of staining. Three separate staining patterns were analyzed: cytoplasmic staining, perinuclear staining, and nuclear staining. The immunoreactive score was chosen to grade the samples. This score considers the number of stained cells and the intensity of staining, where the final score is comprised between 0 and 12. Statistics were performed by using the SPSS software (IBM). Spearman correlation between the two independent scorers was 0.935, $P < 0.0001$. Mann-Whitney U test was used to show significant differences between conditions: cytoplasmic normal versus cytoplasmic lymphomas, $U = 740$, $P < 0.0001$ (sig < 0.05 two-tailed), showing a statistically significant difference between both conditions; nuclear normal versus nuclear lymphomas, $U = 1,115.5$, $P < 0.009$ (sig < 0.05 two-tailed), showing a significant difference; and perinuclear normal versus perinuclear lymphomas, $U = 1291$, $P < 0.257$ (sig < 0.05 two-tailed), showing no significant difference for perinuclear staining. Correlations in expression between pSOCS1 staining and pSRC family staining were calculated using Pearson correlation [Pearson correlation = 0.557, $P < 0.0001$ (sig < 0.01 two-tailed)].

Mass spectrometry

Twenty micrograms of proteins were separated on a 4%–12% precast NuPAGE gel (Invitrogen). The gel was Coomassie-stained with 0.1% Coomassie R250 (B7920, Sigma) in 40% methanol/10% acetic acid. Gel pieces were destained in ACN 50%, reswelled in 50 mmol/L ammonium acetate (Sigma), and reduced with 5 mmol/L tris (2-carboxyethyl)phosphine (TCEP; Pierce). Alkylation was performed by adding chloroacetamide to a final concentration of 55 mmol/L. One microgram of Asp-N was added and the digestion was performed for 4 hours. One microgram of trypsin was added and the digestion was carried out overnight. Peptide extraction was performed with 90% acetonitrile. Samples were dried down in a Speed-Vac and reconstituted in 40 μ L of formic acid (0.2%).

Peptides were loaded on a C18 stem trap from New Objective and separated on a home-made C18 column (15 cm \times 150 μ m id) at a flow rate of 600 nL/minute with a gradient of 5%–30% of acetonitrile (buffer B). Reverse-phase solvents were: buffer A (formic acid 0.2%) and buffer B (formic acid 0.2% in acetonitrile). The analytical column was coupled to a Q-Exactive Plus (Thermo Fisher Scientific). The resolution was set at 70,000 for the survey scan and 17,500 for the tandem mass spectrum acquisition. A maximum of 12 precursors were sequenced for each duty cycle. AGC target values for MS and MS/MS scans were set to 3e6 (max fill time 50 ms) and 2e4 (max fill time 150 ms), respectively. The precursor isolation window was set to m/z 1.6 with a high-energy dissociation normalized collision energy of 25. The dynamic exclusion window was set to 30 seconds. Tandem mass spectra were searched against the UniProt mouse database using PEAKS 7.0 with carbamidomethylation (C) as fixed modifications, deamidation (NQ) oxidation (M) acetylation (N-term), and phosphorylation (STY) as variable modifications. Tolerance was set at 10 ppm on precursor mass and 0.01 kDa on the

Table 3. Missed cleavages

Missed cleavages	0	1	2	3	4+
Sample 1	59	7	0	0	0
Sample 2	127	13	2	0	0
Sample 3	62	10	1	2	0

fragments. Missed cleavages were in low proportion and are given in Table 3.

Proximity ligation assay

SU-DHL4 cells (7×10^6) were seeded at 5.83×10^5 cells/mL and treated with either 12.5 μ mol/L PRIMA-1 (catalog no. A13581, Adooq Bioscience) for 24 hours, 200 nmol/L dasatinib (catalog no. S1021, Selleckchem) for 6 hours or with both compounds. Cells were harvested and fixed in suspension with PFA 4% at 37°C for 10 minutes. In parallel, an area of 1 cm² was delimited with a pap-pen (Liquid blocker super pap-pen), coated with FBS (Wisent), and allowed to air dry. Fixed cells were resuspended in 1 \times PBS/20% FBS (Wisent), applied to the serum-coated area and allowed to deposit for 10 minutes. Then, slides were centrifuged at 800 \times g for 5 minutes and permeabilized with 0.1% Triton X-100 (BioShop) for 15 minutes at room temperature. Cells were washed twice for 5 minutes with 1 \times PBS and then blocked with the blocking solution (Duolink In Situ PLA probes kit, catalog no. DUO92001 or catalog no. DUO92005) for 1 hour at 37°C. Then, cells were incubated with primary antibodies in antibody diluent (Duolink In Situ PLA probes kit) overnight at 4°C. Antibodies were: anti-SOCS1 mouse monoclonal (1:100, clone 4H1, catalog no. K0175, MBL Life Science) and/or anti-p53 rabbit polyclonal (1:1,000, catalog no. A300-247A, Bethyl Laboratories). Cells were washed twice with wash buffer A (catalog no. DUO-82049, Sigma-Aldrich) for 5 minutes followed by an incubation with probe-conjugated secondary antibody in antibody diluent. Probe-conjugated secondary antibodies used for the proximity ligation assay (PLA) experiment: Duolink In Situ PLA Probe Anti-Mouse PLUS (catalog no. DUO92001, Sigma-Aldrich) and Anti-Rabbit MINUS (catalog no. DUO92005, Sigma-Aldrich) with the detection reagents Green (catalog no. DUO92014, Sigma-Aldrich). The ligation and amplification steps were carried as detailed in the manufacturer's protocol from the detection reagents Green kit. Cells were finally washed twice for 10 minutes with 1 \times wash buffer B (catalog no. DUO-82049, Sigma-Aldrich) and once for 1 minute with 0.01 \times wash buffer B. Slides were mounted with ProLong Gold with DAPI (Molecular Probes). Images were acquired with a Zeiss Axio Imager Z2 upright microscope with a Prime sCMOS Camera (Photometrics) and ZEN 2 Imager (version 2.0.14283.302), using the EC Plan-Neofluar 100 \times /1.3 Oil Pol M27 objective.

Additional methods

For details, see Supplementary Information

Results

SOCS1 interacts with a hydrophobic motif found in the transcriptional activation domain 2 of p53 and other transcription factors

We sought to get more insights into the mechanisms by which SOCS1 binds and regulates p53 (3, 5–7). The SH2 domain of SOCS1 constitutes a protein–protein interaction domain allowing target recognition. Previous work concluded that the SH2 domain of SOCS1 (residues 79–170) mediates the interaction

with the N-terminal domain of p53 (residues 1–72; ref. 3). The N-terminus of p53 contains two tandem transcriptional activation domains known as TAD1 (residues 1–34) and TAD2 (residues 35–67). Using GST pull-down assays and ³⁵S-labeled SOCS1 produced by *in vitro* translation, we found that p53 interacts with SOCS1 via the TAD2 (Fig. 1A). The p53 TAD2 binds to the pleckstrin homology (PH) domain of the general transcription factor GTF2H1 (also named p62) using three hydrophobic residues (F54, W53, and I50) and two acidic residues (E51 and E56; ref. 30). It also contains an important phosphorylation site (S46) that regulates p53-dependent gene expression and enhances binding to both p62 and Tfb1 (30). Mutations in S46 or S46 combined with E51 or E56 did not significantly alter the binding of the p53 TAD2 to SOCS1 in GST pull-down assays (Fig. 1B). However, changing W53 to S or F54 to S strongly reduced the binding between the TAD2 and SOCS1 while changing all three residues 50–52 (I-E-N) to A did not inhibit the binding (Fig. 1B).

The TAD2 of p53 shares a structural similarity to many other transcriptional activation domains (Supplementary Fig. S1A), suggesting that SOCS1 may also modulate other transcription factors containing similar hydrophobic motifs. SOCS1 was reported to bind NFκB (31) and KAP1 (32) and we show here that it also binds p73 (Supplementary Fig. S1B). The biological significance of SOCS1 binding to transcription factors may depend on context and imply the presence of a specific domain in SOCS1 that binds and modulates transcriptional activation domains.

A novel interaction pocket in the SH2 domain of SOCS1 mediates interaction with p53

The interaction of SOCS1 with p53 required the SH2 domain of SOCS1 (3), which is proposed to recognize phosphotyrosine-containing motifs via its conserved arginine at position 105 (104 in human; ref. 33). However, the p53 TAD2 does not contain tyrosine and R105K SOCS1 mutant was still able to bind and activate p53 (3). In addition to R105, other positively charged residues of SOCS1 may assist phosphotyrosine binding (34). Still, the mutants R110A, R128A, K119A, and K119E were able to bind p53 (Fig. 1C). The SH2 domain of SOCS1 has an N-terminal extension of 24 residues that are also important for binding to JAK2 (35). Intriguingly, several point mutations and deletions toward the end of this region were found in DLBCL and Hodgkin disease, including amino acid substitutions of F79, Y80, and W81 (Supplementary Fig. S2A). We recreated some of these mutations and found that the mutants of SOCS1 Y80D, Y80S, W81R, and the double mutant 79C/81R all lost their ability to interact with p53 (Fig. 1D). SOCS1 also interacts with tyrosine phosphorylated JAK2 (36), inhibiting JAK2-dependent STAT1 phosphorylation in response to interferon stimulation. We found that wild-type SOCS1 reduces STAT1 phosphorylation while most of the mutants in the SH2 domain N-terminal extension were defective (Supplementary Fig. S3A–B), indicating that the region around Y80 also controls this event.

Consistent with the p53 dependence of SOCS1 antiproliferative effects (3), SOCS1 mutants that cannot bind p53 lost their ability to inhibit cell proliferation in U2OS cells (Fig. 1E). As expected, neither SOCS1 nor the mutants G78S, Y80D, or W81R inhibited growth in p53-null H1299 cells (Supplementary Fig. S3C and S3D). In contrast, the mutant SOCS1 Y80F inhibited colony formation in U2OS cells in a comparable manner with

wild-type SOCS1, while conserving its ability to bind to p53 (Supplementary Fig. S3E and S3F). Next, we studied the ability of SOCS1 to cooperate with the DNA-damaging drug doxorubicin to activate a luciferase reporter with the p53-responsive p21 promoter. We found that the phosphomimetic SOCS1 Y80D mutant was not able to cooperate with doxorubicin to stimulate transcription from this promoter (Fig. 1F–G). Taken together, these results indicate that the region of SOCS1 containing amino acids Y80 and W81 mediates binding to p53 and its functional activation, and that a phosphomimetic substitution of SOCS1 at Y80 inhibits this function.

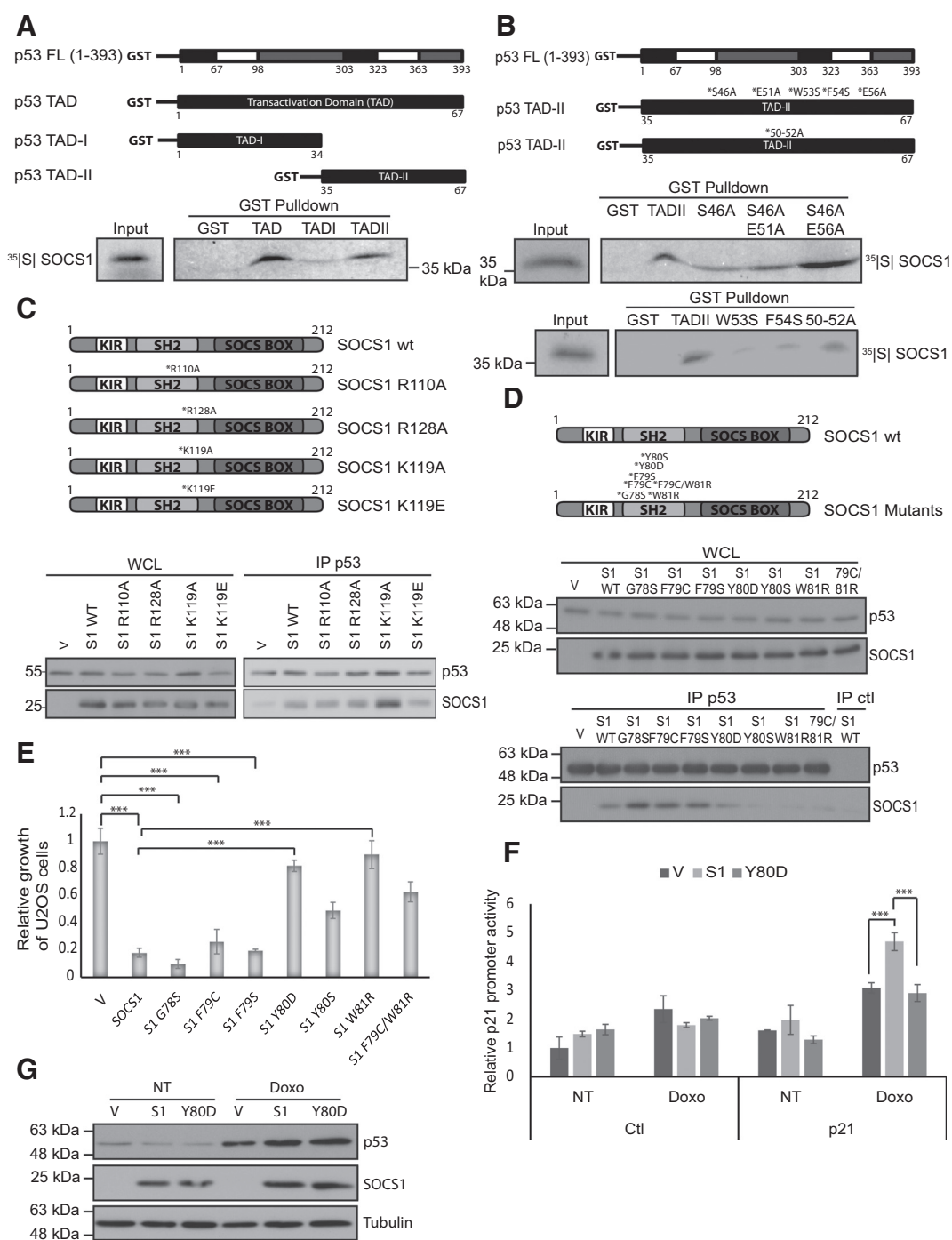
Subsequently, we investigated whether SOCS1 mutations that inhibit p53 binding also reduce its ability to induce p53-dependent senescence in normal human fibroblasts. Expression of SOCS1 in normal human fibroblasts IMR90 induced senescence but knockdown of p53 with a specific shRNA totally prevented the effect (Fig. 2A–C). The SOCS1-mutant Y80D was defective in inducing senescence (Fig. 2A) and growth arrest (Fig. 2C), while the mutant SOCS1 Y80F behaved as the wild-type (Fig. 2A–C). Quantification of the effects of SOCS1 wild-type and Y80 mutants on additional senescence markers show significant defects in the ability of SOCS1 Y80D to induce the senescence biomarkers α -fucosidase (*FUCA*; ref. 37) and *Serpin E1* (38) and the p53 target genes *p21* and *GADD45A* (Fig. 2D–G). Consistent with previous work (3), the ability of wild-type SOCS1 to induce senescence correlated with the stimulation of phosphorylation of p53 on serine 15. However, the mutant SOCS1Y80D lost this ability, while it was retained by the Y80F mutant (Fig. 2H). In summary, the p53-dependent pro-senescent function of SOCS1 is inhibited by a phosphomimetic mutation of the p53-interacting pocket of SOCS1.

SOCS1 is phosphorylated at Y80 by SRC family kinases

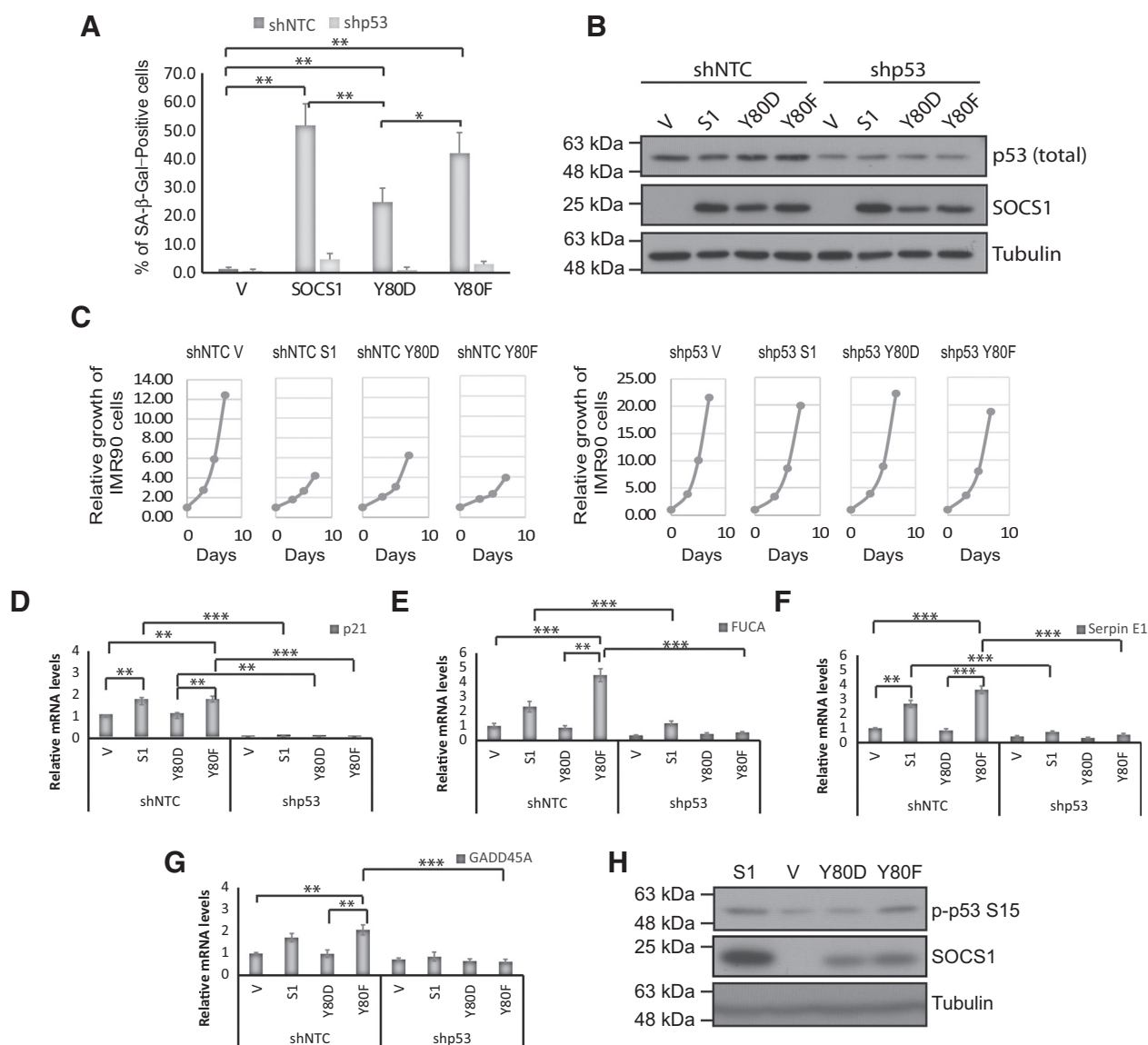
To investigate whether SOCS1 is phosphorylated at Y80, we incubated purified mouse SOCS1 with whole-cell lysates from three different cell types (BV173, HepG2, and IMR90) and then performed mass spectrometry on the SOCS1 protein band obtained after SDS-PAGE. The analyzed peptides included peptides phosphorylated on Y80 as indicated with the mass spectra in Fig. 3A. The sequence of the identified phosphorylated peptide is shown in Fig. 3B.

To identify candidate kinases that can phosphorylate SOCS1 and inhibit its interaction with p53, we used a bank of activated tyrosine kinases pooled in five groups of 4–5 kinases each. Kinases in group 1 reduced p53–SOCS1 interaction (Fig. 3C) and were further analyzed. Among the kinases in this group, the SRC family kinase YES1 appreciably reduced p53–SOCS1 interaction (Fig. 3D). Also, endogenous YES1 coimmunoprecipitated with SOCS1 in U2OS cells overexpressing SOCS1 (Fig. 3E). To further investigate the implication of SRC family kinases in SOCS1 phosphorylation at Y80, we generated a mAb capable of recognizing SOCS1 phosphorylated at Y80. To validate this antibody, we first stimulated wild-type or SOCS1-null MEFs with EGF and performed IHC. We could detect a strong signal in wild-type MEFs stimulated with EGF, but not in SOCS1-null MEFs under similar conditions (Fig. 3F). Next, we used purified SOCS1 and performed *in vitro* kinase assays with either YES1 or the related kinase SRC. The antibody recognized SOCS1 in immunoblots after incubation of SOCS1 with these kinases in the presence of ATP and the signal was decreased by the mutation of Y80F (Fig. 3G). Interestingly, after *in vitro* phosphorylation reactions, SOCS1

Saint-Germain et al.

**Figure 1.**

Identification of a novel interaction mechanism between SOCS1 and p53. **A-D**, Each panel shows a schematic representation of the GST-p53 fusion proteins (**A** and **B**) or of SOCS1 variants (**C** and **D**) and the resulting *in vitro* interaction between SOCS1 and p53. Mutations are indicated by an * followed by the corresponding amino acid change. **A**, Interaction of ^{35}S labeled-SOCS1 with GST-p53 TAD, GST-p53 TAD-I, and GST-p53 TAD-II. **B**, Interaction of ^{35}S labeled-SOCS1 with GST-p53 TADII mutants of hydrophobic residues. **C**, SOCS1 (S1) does not interact with p53 via the same amino acids with which it interacts with JAKs. Coimmunoprecipitation of p53 or control IP (anti-Cyclin A: IP CA) was performed in U2OS cells transiently transfected with the SOCS1 wild-type (S1 WT) or mutants and treated with doxorubicin (300 ng/mL) for 16 hours. Lysates and immunoprecipitates were immunoblotted for the indicated proteins. WCL, whole-cell lysates; V, control vector. **D**, SOCS1-p53 interaction is decreased when SOCS1 is mutated on Y80 or W81. Coimmunoprecipitation was performed in U2OS as described in **C**. **E**, SOCS1 mutated on Y80 or W81 loses its ability to arrest growth of cancer cells. Colony assays were performed in U2OS cells transiently transfected with the various constructs described in **D**. **F**, Luciferase assays in U2OS cells cotransfected with pGL3-promoter control vector (Ctl) or pGL3 p21-promoter vector in combination with a control vector (V), a vector expressing SOCS1 (S1), or a SOCS1 mutant for Y80D. Cells were either untreated (NT) or treated with 300 ng/mL doxorubicin (Doxo) for 24 hours. **G**, Western blots showing the levels of p53 and SOCS1 in cells as in **F**. Tubulin was used as loading control. ***, $P < 0.005$.

**Figure 2.**

SOCS1 phosphomimetic and unphosphorylatable mutants impact cellular senescence in normal human fibroblasts. **A**, Senescence-associated β -galactosidase assay (SA- β -gal) of cells expressing an empty vector (V), wild-type SOCS1 (SOCS1wt), SOCS1 Y80D, or SOCS1 Y80F in combination with either a nontargeting shRNA (shNTC) or a shRNA against p53 (shp53). **B**, Immunoblots of indicated proteins performed on cells as in **A**. **C**, Growth curves of IMR90 cells as in **A**. Data are presented as means normalized to day 0 of each condition. S1, SOCS1 wild-type. **D–G**, qPCR for the indicated genes performed on reverse transcribed total RNA extracted from cells as in **A**. **H**, Immunoblots of the indicated proteins showing that SOCS1 mutation Y80D loses its ability to stimulate p53 phosphorylation. IMR90 cells were infected with empty vector (V) or derivatives expressing wild-type SOCS1 (S1), SOCS1 Y80D, or SOCS1 Y80F. All experiments were performed three times; error bars indicate the SD of triplicates. *, $P < 0.05$, using two tailed Student t test; **, $P < 0.01$; ***, $P < 0.005$.

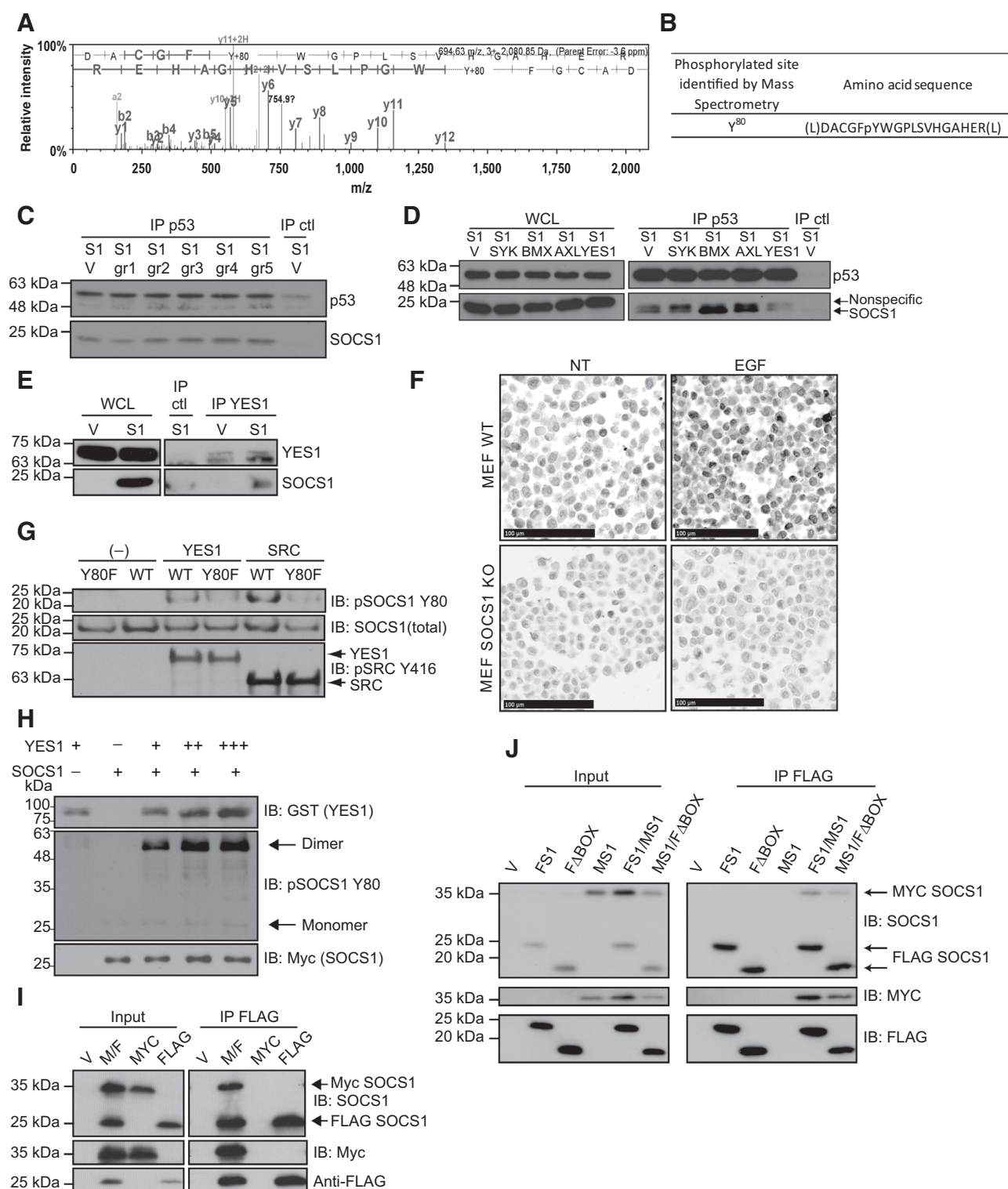
migrated at a molecular weight corresponding to a dimer unless the protein extracts were heated in 8 mol/L urea (Fig. 3H), suggesting that phospho-SOCS1 efficiently forms very stable dimers or that mainly SOCS1 dimers are phosphorylated by YES1. We confirmed that this dimeric form of SOCS1 exists in cells by doing a coimmunoprecipitation between a FLAG-tagged SOCS1 and a MYC-tagged SOCS1 (Fig. 3I). Moreover, a mutant of SOCS1 without the SOCS box domain tagged with FLAG was able to interact with MYC-tagged SOCS1, indicating that the SH2

domain is sufficient for dimerization (Fig. 3J). We conclude that the SRC family kinase phosphorylates SOCS1 on Y80 inhibiting its interaction with p53 and favoring the formation of SOCS1 dimers.

SRC family kinase inhibitors potentiate p53 activation and senescence in SOCS1-expressing cells

SRC family kinase (SFK) inhibitors have been developed and are under clinical evaluation as cancer therapeutics (39).

Saint-Germain et al.

**Figure 3.**

SOCS1 is phosphorylated on Y80 by SRC family kinase members SRC and YES1. **A**, Mass spectra obtained for a typical peptide showing phosphorylation of Y80. Whole-cell lysates from three cell lines (IMR90, HepG2, and BV173) were each incubated with *in vitro* purified GST-SOCS1 to test whether phosphorylation occurs in different cell types. Extracts were then loaded onto an SDS-PAGE gel and the band corresponding to SOCS1 was analyzed by mass spectrometry. **B**, Sequence of the phosphorylated peptide identified by mass spectrometry. **C**, Immunoblots of indicated proteins following coimmunoprecipitation of SOCS1 (S1) with p53 in cells expressing a control vector (V) or pools of activated tyrosine kinases (gr1-gr5). (Continued on the following page.)

These inhibitors could potentially reactivate the SOCS1-p53 pathway in tumors overexpressing SOCS1, triggering anti-tumor responses. First, we confirmed that SFK inhibitors could block the phosphorylation of SOCS1 by SRC in an *in vitro* kinase assay using purified SOCS1 incubated with SRC kinase and different concentrations of dasatinib (4 nmol/L or 100 nmol/L). SOCS1 was phosphorylated in the absence of dasatinib, but the drug strongly decreased SOCS1 phosphorylation at a concentration of 100 nmol/L (Fig. 4A). To investigate whether SFK inhibitors can potentiate the SOCS1-p53 pathway, we first evaluated their effect on p53-dependent senescence triggered by SOCS1 in normal human fibroblasts. Introduction of SOCS1 in IMR90 cells reduced cell growth and induced senescence, turning around 40% of the cells SA- β -gal positive (Fig. 4B). Combining SOCS1 with 20 nmol/L or higher of SFK inhibitors dasatinib or saracatinib increased the percentage of senescent cells (Fig. 4B). This effect correlated with higher levels of serine 15 phosphorylation of p53 (Fig. 4C). The reinforcement of SOCS1-induced senescence translated into an improvement of the growth arrest induced by SOCS1 in the cell population (Fig. 4D). We also found that SFK inhibitors did not reinforce senescence induced by a mutant of SOCS1 that cannot be phosphorylated at Y80 (Fig. 4E). Hence, the cooperation of SOCS1 with SFK inhibitors depended on Y80.

SOCS1 is phosphorylated at Y80 in human cancers

The presence of SOCS1 mutations in some patients with DLBCL and Hodgkin disease is consistent with a tumor suppressor role for SOCS1 in these cancers. However, gene expression analysis revealed an unexpected increase in SOCS1 expression in DLBCL, Burkitt lymphoma, and follicular lymphoma (Fig. 5A and B; Supplementary Fig. S4A). This is surprising because p53 mutations are not common in DLBCL (Supplementary Fig. S4B) and SOCS1 could activate p53 and halt tumor progression. In fact, SOCS1 and p53 mutations are mutually exclusive along several types of cancers signifying that they act in a common pathway (Supplementary Fig. S4C). We thus reasoned that for most cases of DLBCL that overexpress SOCS1, SOCS1 Y80 phosphorylation could avoid p53 activation. Consistent with this idea, YES1, the SRC family kinase we identified in our SOCS1 Y80 kinase screen, is highly expressed in DLBCL (Supplementary Fig. S4D). To investigate whether SOCS1 phosphorylation at Y80 is increased in DLBCL, we performed IHC in tissue microarrays containing samples from

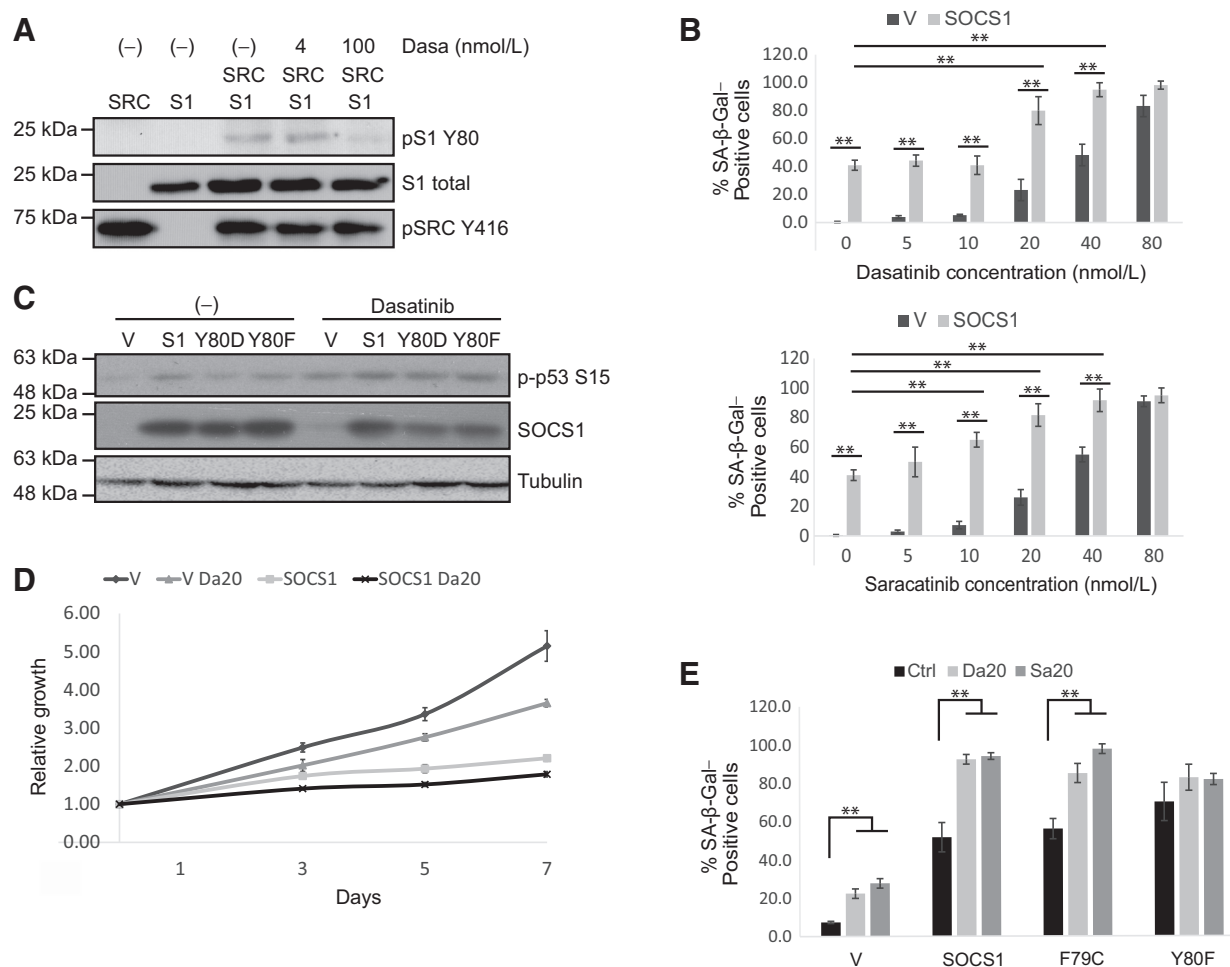
several patients with lymphoma (Supplementary Fig. S5A). We identified four degrees of staining (negative, mild, moderate, and strong; Fig. 5C) in three different cellular compartments (nuclear, perinuclear, and cytoplasmic; Supplementary Fig. S5B). We found a high percentage of strong and moderate cytoplasmic and perinuclear staining in DLBCL and other lymphomas, while normal lymph nodes never stained strong and have a higher percentage of moderate nuclear staining (Fig. 5D and E). These results are consistent with the idea that SOCS1 phosphorylation at Y80 acts as an oncogenic modification that avoids the tumor suppressor functions of SOCS1.

Next, we studied the status of the SRC family kinase in the same tissue microarrays using an antibody that reacts with activated SRC family members. We found that in general, lymphomas stained positive for these kinases while normal tissues were mostly negative (Fig. 6A and B). In addition, there was a significant correlation between the staining for activated SRC family and for SOCS1 phosphorylation at Y80 (Pearson correlation 0.557). Because B cells and their neoplasias express high levels of several SRC-family kinases, we investigated whether LCK, LYN, and BLK could phosphorylate SOCS1 at Y80. We found that these kinases were all able to phosphorylate SOCS1 at Y80 to different levels (Fig. 6C). Of note, BLK and LYN expression is higher in DLBCL than either YES1 or SRC, although there is a large variability in the expression of these kinases at the mRNA level (Supplementary Fig. S6A-S6D). These results imply that to restore SOCS1 tumor suppression activity in DLBCL, drugs should efficiently target B-cell-specific SRC family members.

Finally, to demonstrate that drugs targeting SRC family kinases can reactivate the SOCS1-p53 axis in B-cell lymphoma cells, we used the B-cell lymphoma cell line SU-DHL4. These cells express both SOCS1 and a mutant p53 allele (R273C) that can be reactivated by the compound PRIMA-1, which binds covalently to the core domain of p53 (40). To capture the complex between p53 and SOCS1 in these tumor cells after treatment with dasatinib, we used the proximity ligation assay (Duolink), which is more sensitive than coimmunoprecipitation to detect protein interactions at endogenous levels. Dasatinib alone did not significantly increase p53-SOCS1 interactions as measured by this assay. However, upon reactivation of endogenous p53 with PRIMA-1, we were able to reveal numerous foci representing p53-SOCS1 complexes in these cells (Fig. 6D and E; Supplementary Fig. S7). Together, these results

(Continued.) Group 1 (AXL, BMX, SYK, and YES1), group 2 (TEC, LCK, TYK2, BTK), group 3 (FGFR1, HCK, TNK2, and EphA4), group 4 (BLK, FRK, TIE1, and FGR), and group 5 (MATH, ITK, and RET). **D**, YES1 kinase overexpression decreases the interaction between p53 and SOCS1. Immunoblots showing coimmunoprecipitation of SOCS1 (S1) with p53 in cells expressing a control vector (V) or each of the kinases of group 1. WCL, whole-cell lysates. **E**, YES1 and SOCS1 interact together. Whole-cell lysates and immunoprecipitates were immunoblotted for indicated proteins following immunoprecipitation of YES1 or control (ctl) in U2OS cells overexpressing SOCS1 (S1) or a control vector (V). **F**, Validation of a novel antibody against phospho-Y80 SOCS1 by IHC on wild-type MEFs or SOCS1 knockout MEFs either untreated or stimulated with EGF following serum starvation. **G**, *In vitro* kinase assay shows that GST-YES1 and SRC-His phosphorylate SOCS1. Active GST-YES1 and SRC-His were incubated with purified FLAG-SOCS1 wild-type (WT) or FLAG-SOCS1 Y80F *in vitro*. After denaturation in 8 mol/L urea, phosphorylation was assessed by Western blot with the mAb specific to phosphorylated SOCS1 at Y80 (pSOCS1 Y80). SRC kinases are detected with phospho-SRC Y416 (pSRC Y416). **H**, Majority of phosphorylated SOCS1-Myc-FLAG is found as a dimer when no denaturation in 8 mol/L urea is used. Immunoblots of GST-YES1, SOCS1-Myc-Flag, and phospho-SOCS1 (pSOCS1 Y80) of *in vitro* kinase assays using purified SOCS1-Myc-FLAG and increasing concentrations of purified GST-YES1 in absence of urea. **I**, SOCS1 dimerizes in cells. U2OS cells were transfected with empty vector (V), 6 \times MYC-SOCS1, and FLAG-SOCS1 (M/F), 6 \times MYC-SOCS1 alone (MYC) or FLAG-SOCS1 alone (FLAG) and immunoprecipitated with an anti-FLAG antibody. Lysates (Input) and immunoprecipitates were immunoblotted for the indicated proteins. **J**, SOCS1 SH2 domain is sufficient for dimerization. U2OS cells were transfected with control vector (V), different combinations of 6 \times MYC-SOCS1 (MS1) and FLAG-SOCS1 (FS1) or FLAG-SOCS1 Δ BOX (F Δ BOX) and immunoprecipitated with an anti-FLAG antibody. Lysates and immunoprecipitates were immunoblotted for indicated proteins.

Saint-Germain et al.

**Figure 4.**

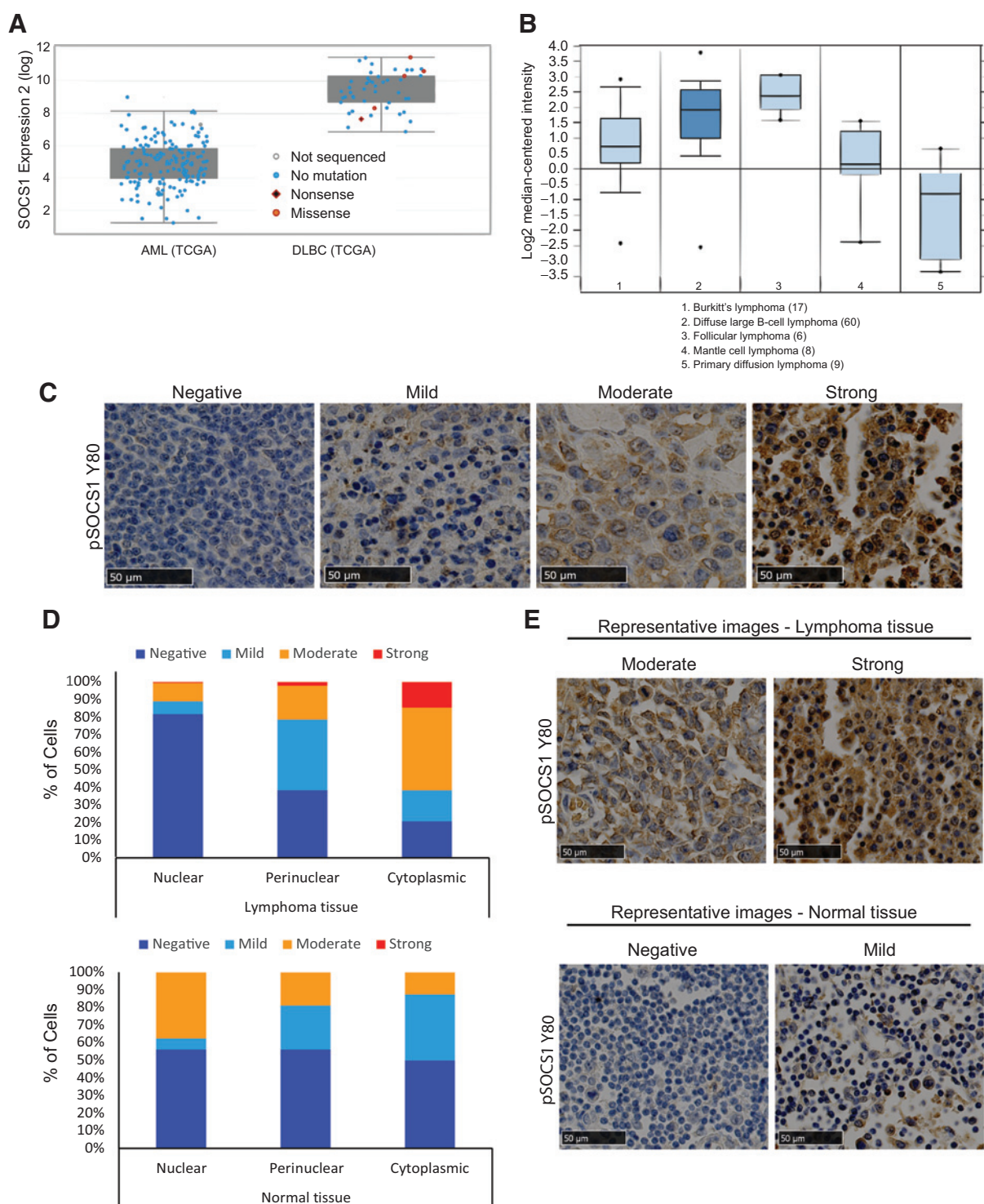
Inhibiting the SRC family enhances SOCS1 tumor suppressor activity. **A**, Dasatinib inhibits SOCS1 phosphorylation in *in vitro* kinase assays. Kinase assay was performed as described previously using purified proteins but adding to the reaction the SRC inhibitor dasatinib at either 4 nmol/L or 100 nmol/L. S1, SOCS1; pS1 Y80, phospho-SOCS1 Y80; pSRC Y416, phospho-SRC family Y416. **B**, SRC family inhibitors cooperate with SOCS1 to induce a stronger senescence. IMR90 cells infected with an empty vector (V) or SOCS1 were treated with increasing doses of dasatinib (top) or saracatinib (bottom), ranging from 0 to 80 nmol/L for one week. Senescence-associated- β -galactosidase (SA- β -gal) staining was then performed to quantify the number of senescent cells. **C**, Immunoblots for the indicated proteins on cell lysates from IMR90 cells infected with empty vector (V), wild-type SOCS1 (S1), SOCS1 Y80D, or SOCS1 Y80F and treated or not with 100 nmol/L dasatinib for 24 hours. P-p53 S15, phosphorylated p53 at serine 15. **D**, IMR90 cells infected with an empty vector (V) or SOCS1 were treated with 20 nmol/L dasatinib (Da20) for one week, the dose showing the best effect in **B** before being counted and plated for a growth curve. **E**, SA- β -gal staining in cells expressing either a control vector (V), wild-type SOCS1, or SOCS1 mutants F79C or Y80F and treated with dasatinib 20 nmol/L (Da20) or saracatinib 20 nmol/L (Sa20). All experiments were performed three times; error bars indicate the SD of triplicates. **, $P < 0.01$, using one-way ANOVA followed by Tukey HSD test (**B**) or the Student *t* test (**E**).

show that SRC family kinase inhibitors can reactivate the SOCS1-p53 tumor suppressor axis when used alone in cells with wild-type p53 or in combination with compounds that can reactivate mutant p53 in cells that express such mutants.

Discussion

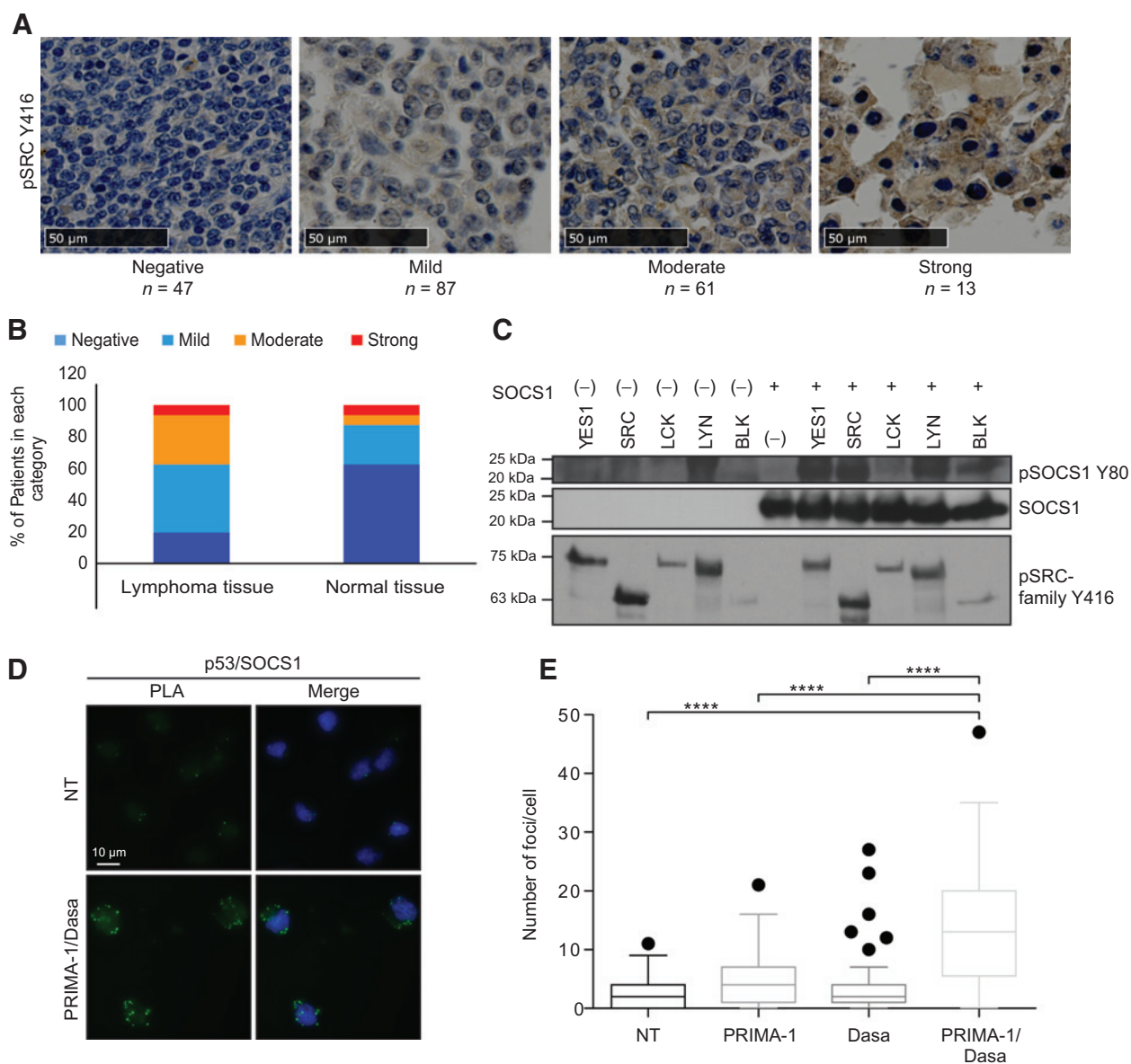
Tumor suppressors are often disabled in cancer cells by mutations or expression silencing. However, cancer cells over-express enzymes that catalyze protein posttranslational mod-

ifications, some of which could also inactivate tumor suppressors (41). Here, we report that the functions of the tumor suppressor SOCS1 are inhibited by phosphorylation on Y80 catalyzed by the SRC family of protein tyrosine kinases. We found that Y80 in SOCS1 is part of a motif that mediates interaction with p53. Mutations in this motif are found with low frequency in human cancers where paradoxically most patients display high levels of SOCS1 expression. Our analysis of samples from several cases of human lymphomas indicates a frequent SOCS1 phosphorylation on Y80, suggesting a

**Figure 5.**

Phosphorylated SOCS1 at Y80 is deregulated in human DLBCL. **A**, SOCS1 expression levels (RNA-seq data from cBioPortal) in two types of hematopoietic cancers, acute myeloid leukemia (AML) and DLBCL. **B**, OncoPrint analysis of SOCS1 expression levels in different types of lymphomas shows DLBCL lymphomas have among the highest expression levels of SOCS1. **C**, Scale of staining intensity calculated with the immunoreactivity scoring method for phosphorylated SOCS1 Y80 in IHC on tissue microarrays of human DLBCL patients (LY2086a, US Biomax). **D**, Staining of pSOCS1 Y80 is increased in the cytoplasm of lymphoma tissues compared with normal lymph nodes. Analysis of pSOCS1 Y80 staining in human DLBCL samples from the tissue microarrays (LY2086a). Top, lymphoma tissues; bottom, normal lymph nodes. Nuclear, perinuclear, and cytoplasmic staining were analyzed and quantified. Results are shown in graphics comparing the percentage of cells stained in each category and the intensity of staining. **E**, Images of the most representative phenotypes obtained in patients with DLBCL (top) and normal lymph nodes (bottom) for pSOCS1 Y80.

Saint-Germain et al.

**Figure 6.**

SRC family kinases phosphorylate SOCS1 on Y80 and inhibit endogenous SOCS1-p53 interaction in lymphomas. **A**, Example of the four different categories of staining defined for pSRC-family Y416 (pSRC Y416): negative, mild, moderate, and strong. Number of samples staining for each category is indicated. **B**, Comparison of relative number of patients staining in each category is shown for lymphoma samples versus normal lymph nodes. Lymphomas stain more strongly for pSRC staining. **C**, Kinase assays using SRC family members important in B or T cells (LYN, BLK, and LCK) compared with YES1 and SRC were performed to compare levels of monomeric phosphorylated SOCS1. After kinase reactions, extracts were heated in 8 mol/L urea to visualize monomeric SOCS1. **D**, PLA for SOCS1 and p53 in SU-DHL4 cells following treatments with the combination of 12.5 μ mol/L PRIMA-1 for 24 hours and 200 nmol/L dasatinib (Dasa) for 6 hours. Not treated (NT) cells were used as controls. Scale bar, 10 μ m. DAPI DNA counterstain is visualized in the merge images. **E**, PLA quantification of the number of foci per cell for SU-DHL4 cells treated with PRIMA-1, dasatinib (Dasa), or both compounds and compared with nontreated cells. The box plots represent the combination of the counts of foci from 45 cells, 15 cells from each of three independent experiments. Each box plot shows median number of PLA foci; boxes and whiskers were determined using the Tukey whisker method. ****, $P < 0.0001$, using one-sided ANOVA test.

mechanism that explains why these tumors retain high levels of SOCS1.

The SH2 domain is a phosphotyrosine-binding module originally described in the SRC family of tyrosine kinases (42). The motif that mediates the interaction between SOCS1 and p53 includes Y80 and W81 and is located at the N-terminal

extension of the SH2 domain of SOCS1. This motif is conserved in other SOCS family proteins, including SOCS3, which also binds to p53 (43). The tertiary structure of the SH2 domain of SOCS3 shows that the extended SH2 subdomain forms an amphipathic helix, with the hydrophobic side binding the phospho-tyrosine binding loop of the SH2

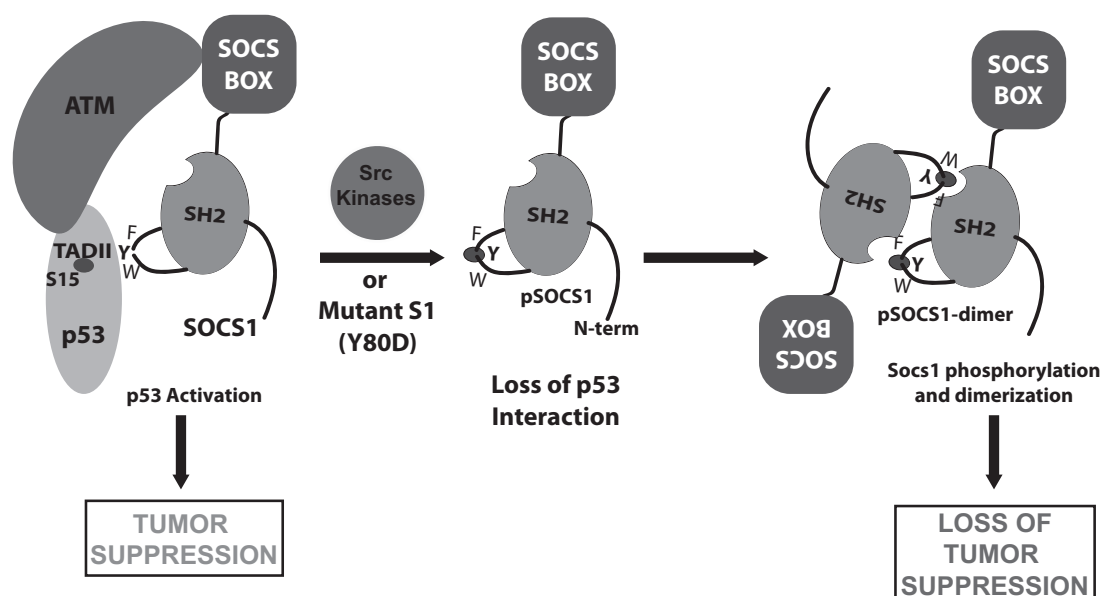


Figure 7.

Model showing the role of mutations and phosphorylation on the tumor suppressor role of SOCS1 in the p53 pathway. SOCS1 binds p53, facilitating its ATM-dependent phosphorylation on serine 15. SRC kinases phosphorylate SOCS1 on Y80, inhibiting its interaction with p53 and promoting SOCS1 dimerization. SOCS1 dimers are proposed to occur by recognition of phospho-Y80 by the phosphotyrosine binding motif in the SH2 domain of SOCS1.

domain (44). Y47 and W48 of SOCS3 (Y80 and W81 in SOCS1) lie to the C-terminal part of the extended subdomain forming a loop exposed to the protein surface (34, 44). Additional structural work will be required to characterize the noncanonical binding of SOCS1 to p53, which does not require phosphorylated tyrosine and binds hydrophobic patches present in the amphipathic alpha helix of the TAD2 of p53. Phosphorylation of Y80 in SOCS1 could interfere with protein-protein interactions directly via the negative charge of the phosphate or by preventing Y-mediated contacts with the interaction partner. It is also possible that phosphorylation on Y80 induces conformational changes in SOCS1 that disables its binding to other proteins. In particular, phospho-Y80 could bind the phosphotyrosine binding pocket of the same molecule of SOCS1 or bind to another SOCS1 molecule to form inactive dimers as our results suggest. Of note, SOCS1 Y80D mutant was unable to bind p53 or inhibit STAT1 phosphorylation in response to interferon, suggesting that tyrosine phosphorylation of SOCS1 at Y80 is a general mechanism to control its activity (Fig. 7).

Furthermore, previous studies have identified phosphorylation as a means of negative regulation of SOCS1. One group identified the fusion protein BCR-ABL, responsible for chronic myelogenous leukemia, as a SOCS1 kinase (45). Their publication identified Y155 and Y204 of SOCS1 as the main tyrosines phosphorylated by BCR-ABL. Phosphorylation of SOCS1 on these sites prevented the inhibition of the JAK/STAT pathway and mutation of both tyrosines to phenylalanine suppressed tumor growth (46). Their results also show that mouse Socs1 Y80F is less phosphorylated in response to BCR-ABL, indicating that this residue might be a target for this kinase even though they did not further study this particular tyrosine.

Our mass spectrometry results have allowed us to obtain peptides for three of the four tyrosine residues in SOCS1, but Y155 and Y204 were not phosphorylated in the three cell lines we looked at, whereas Y80 was phosphorylated.

Furthermore, in the context of cancer cells, phosphorylation of SOCS1 on Y80 can effectively block its tumor suppression activity. In DLBCL, mutations of SOCS1 and p53 are mutually exclusive (17) but most patients overexpress SOCS1 and have wild-type p53 (Fig. 5A and B; Supplementary Fig. S4). We propose that the SOCS1-p53 axis is mostly disabled by Y80 phosphorylation of SOCS1 in DLBCL and other lymphomas. This idea is supported by our data showing high levels of Y80-phosphorylated SOCS1 in the cytosol of cells from patients with DLBCL and its correlation with high levels of activated SRC-kinases. An important question is whether SRC family kinase inhibitors can be used to reactivate the SOCS1-p53 axis in tumors with constitutive phosphorylation of SOCS1 on Y80. In cell culture, the induction of p53 and senescence by SOCS1 was potentiated by SRC family kinase inhibitors. Also, in the lymphoma cell line SU-DHL4 a, SRC family kinase inhibitor promoted the interaction between SOCS1 and a mutant p53 protein reactivated by the compound PRIMA-1. Previous work found constitutively high SFK expression in B-cell lymphoma cell lines conferring sensitivity to SFK inhibitors (47). Data from Oncomine (Supplementary Fig. S6) show that DLBCLs express high levels of BLK, LYN, and YES1 and we found that these kinases are as efficient as SRC in phosphorylating SOCS1 at Y80. Despite the extensive preclinical evidence linking the SRC family to tumor progression, the results of using SRC family inhibitors in clinical trials have been disappointing in solid tumors (25). One reason for these results is the lack of biomarkers to select patients for

Saint-Germain et al.

treatment. We suggest that SFK inhibitors can be effective in patients that have high levels of Y80 phosphorylated SOCS1 and either wild-type p53 or a mutant p53 that can be pharmacologically reactivated.

Disclosure of Potential Conflicts of Interest

No potential conflicts of interest were disclosed.

Authors' Contributions

Conception and design: E. Saint-Germain, L. Mignacca, V. Calabrese, V. Bourdeau, F. Lessard, G. Ferbeyre

Development of methodology: E. Saint-Germain, L. Mignacca, V. Calabrese, V. Bourdeau, F. Lessard, G. Ferbeyre

Acquisition of data (provided animals, acquired and managed patients, provided facilities, etc.): E. Saint-Germain, L. Mignacca, G. Huot, M. Acevedo, K. Moineau-Vallée, F. Lessard, G. Ferbeyre

Analysis and interpretation of data (e.g., statistical analysis, biostatistics, computational analysis): E. Saint-Germain, L. Mignacca, G. Huot, K. Moineau-Vallée, S. Ilangumaran, F. Lessard, G. Ferbeyre

Writing, review, and/or revision of the manuscript: E. Saint-Germain, V. Bourdeau, S. Ilangumaran, F. Lessard, G. Ferbeyre

Administrative, technical, or material support (i.e., reporting or organizing data, constructing databases): E. Saint-Germain, V. Bourdeau, M.-C. Rowell, G. Ferbeyre

Study supervision: F. Lessard, G. Ferbeyre

Acknowledgments

We thank Scott Lowe (MSK), David Bernard (Cancer Research Centre of Lyon), Caroline Saucier (U. Sherbrooke), James G. Omichinsky (U. Montréal) for comments and/or reagents, and Rémy Beaujois for technical assistance. We also thank all members of the Ferbeyre laboratory for their useful comments. Proteomics analyses were performed by the Center for Advanced Proteomics Analyses, a Node of the Canadian Genomic Innovation Network that is supported by the Canadian Government through Genome Canada. IHC of TMAs was performed at the IRIC Histology Platform. F. Lessard is supported by FRQS (Fonds de Recherche du Québec-Santé) and CRS (Cancer Research Society). G. Ferbeyre is supported by the CIBC chair for breast cancer research at the CRCHUM. This work was funded by a grant from the Canadian Institute of Health and Research (CIHR-MOP229774 to G. Ferbeyre).

The costs of publication of this article were defrayed in part by the payment of page charges. This article must therefore be hereby marked *advertisement* in accordance with 18 U.S.C. Section 1734 solely to indicate this fact.

Received May 15, 2018; revised March 21, 2019; accepted May 13, 2019; published first May 17, 2019.

References

1. Beauvillage C, Champagne A, Tobelaim WS, Pomerleau V, Menendez A, Saucier C. SOCS1 in cancer: an oncogene and a tumor suppressor. *Cytokine* 2016;82:87–94.
2. Kamura T, Sato S, Haque D, Liu L, Kaelin WG Jr., Conaway RC, et al. The Elongin BC complex interacts with the conserved SOCS-box motif present in members of the SOCS, ras, WD-40 repeat, and ankyrin repeat families. *Genes Dev* 1998;12:3872–81.
3. Calabrese V, Mallette FA, Deschenes-Simard X, Ramanathan S, Gagnon J, Moores A, et al. SOCS1 links cytokine signaling to p53 and senescence. *Mol Cell* 2009;36:754–67.
4. Bouamar H, Jiang D, Wang L, Lin AP, Ortega M, Aguiar RC. MicroRNA 155 control of p53 activity is context dependent and mediated by Aicda and Socs1. *Mol Cell Biol* 2015;35:1329–40.
5. Shimada K, Serada S, Fujimoto M, Nomura S, Nakatsuka R, Harada E, et al. Molecular mechanism underlying the antiproliferative effect of suppressor of cytokine signaling-1 in non-small-cell lung cancer cells. *Cancer Sci* 2013;104:1483–91.
6. Mallette FA, Calabrese V, Ilangumaran S, Ferbeyre G. SOCS1, a novel interaction partner of p53 controlling oncogene-induced senescence. *Aging* 2010;2:445–52.
7. Cui X, Shan X, Qian J, Ji Q, Wang L, Wang X, et al. The suppressor of cytokine signaling SOCS1 promotes apoptosis of intestinal epithelial cells via p53 signaling in Crohn's disease. *Exp Mol Pathol* 2016;101:1–11.
8. Zardo G, Tiirikainen MI, Hong C, Misra A, Feuerstein BC, Volik S, et al. Integrated genomic and epigenomic analyses pinpoint biallelic gene inactivation in tumors. *Nat Genet* 2002;32:453–8.
9. Chim CS, Wong KY, Loong F, Srivastava G. SOCS1 and SHP1 hypermethylation in mantle cell lymphoma and follicular lymphoma: implications for epigenetic activation of the Jak/STAT pathway. *Leukemia* 2004;18:356–8.
10. Sutherland KD, Lindeman GJ, Choong DY, Wittlin S, Brentzell L, Phillips W, et al. Differential hypermethylation of SOCS genes in ovarian and breast carcinomas. *Oncogene* 2004;23:7726–33.
11. Hatimaz O, Ure U, Ar C, Akyerli C, Soysal T, Ferhanoglu B, et al. The SOCS-1 gene methylation in chronic myeloid leukemia patients. *Am J Hematol* 2007;82:729–30.
12. Chevrier M, Bobbala D, Villalobos-Hernandez A, Khan MG, Ramanathan S, Saucier C, et al. Expression of SOCS1 and the downstream targets of its putative tumor suppressor functions in prostate cancer. *BMC Cancer* 2017;17:157.
13. Jiang S, Zhang HW, Lu MH, He XH, Li Y, Gu H, et al. MicroRNA-155 functions as an OncomiR in breast cancer by targeting the suppressor of cytokine signaling 1 gene. *Cancer Res* 2010;70:3119–27.
14. Kobayashi N, Uemura H, Nagahama K, Okudela K, Furuya M, Ino Y, et al. Identification of miR-30d as a novel prognostic maker of prostate cancer. *Oncotarget* 2012;3:1455–71.
15. Zhao XD, Zhang W, Liang HJ, Ji WY. Overexpression of miR-155 promotes proliferation and invasion of human laryngeal squamous cell carcinoma via targeting SOCS1 and STAT3. *PLoS one* 2013;8:e56395.
16. Mestre C, Rubio-Moscardo F, Rosenwald A, Climent J, Dyer MJ, Staudt L, et al. Homozygous deletion of SOCS1 in primary mediastinal B-cell lymphoma detected by CGH to BAC microarrays. *Leukemia* 2005;19:1082–4.
17. Reddy A, Zhang J, Davis NS, Moffitt AB, Love CL, Waldrop A, et al. Genetic and functional drivers of diffuse large B cell lymphoma. *Cell* 2017;171:481–94.
18. Lennerz JK, Hoffmann K, Bubolz AM, Lessel D, Welke C, Ruther N, et al. Suppressor of cytokine signaling 1 gene mutation status as a prognostic biomarker in classical Hodgkin lymphoma. *Oncotarget* 2015;6:29097–110.
19. Mottok A, Renne C, Willenbrock K, Hansmann ML, Brauning A. Somatic hypermutation of SOCS1 in lymphocyte-predominant Hodgkin lymphoma is accompanied by high JAK2 expression and activation of STAT6. *Blood* 2007;110:3387–90.
20. Tagami-Nagata N, Serada S, Fujimoto M, Tanemura A, Nakatsuka R, Ohkawara T, et al. Suppressor of cytokine signalling-1 induces significant preclinical antitumor effect in malignant melanoma cells. *Exp Dermatol* 2015;24:864–71.
21. Tobelaim WS, Beauvillage C, Champagne A, Pomerleau V, Simoneau A, Chababi W, et al. Tumour-promoting role of SOCS1 in colorectal cancer cells. *Sci Rep* 2015;5:14301.
22. Reddy PN, Sargin B, Choudhary C, Stein S, Grez M, Muller-Tidow C, et al. SOCS1 cooperates with FLT3-ITD in the development of myeloproliferative disease by promoting the escape from external cytokine control. *Blood* 2012;120:1691–702.
23. Berzaghi R, Maia VS, Pereira FV, Melo FM, Guedes MS, Origassa CS, et al. SOCS1 favors the epithelial-mesenchymal transition in melanoma, promotes tumor progression and prevents antitumor immunity by PD-L1 expression. *Sci Rep* 2017;7:40585.
24. Hanahan D, Weinberg RA. Hallmarks of cancer: the next generation. *Cell* 2011;144:646–74.

25. Zhang S, Yu D. Targeting Src family kinases in anti-cancer therapies: turning promise into triumph. *Trends Pharmacol Sci* 2012;33:122–8.
26. Polonio-Vallon T, Kirkpatrick J, Krijgsveld J, Hofmann TG. Src kinase modulates the apoptotic p53 pathway by altering HIPK2 localization. *Cell Cycle* 2014;13:115–25.
27. Ilangumaran S, Finan D, La Rose J, Raine J, Silverstein A, De Sepulveda P, et al. A positive regulatory role for suppressor of cytokine signaling 1 in IFN-gamma-induced MHC class II expression in fibroblasts. *J Immunol* 2002;169:5010–20.
28. Ferbeyre G, de Stanchina E, Querido E, Baptiste N, Prives C, Lowe SW. PML is induced by oncogenic ras and promotes premature senescence. *Genes Dev* 2000;14:2015–27.
29. Deschenes-Simard X, Gaumont-Leclerc MF, Bourdeau V, Lessard F, Moiseeva O, Forest V, et al. Tumor suppressor activity of the ERK/MAPK pathway by promoting selective protein degradation. *Genes Dev* 2013;27:900–15.
30. Di Lello P, Jenkins LM, Jones TN, Nguyen BD, Hara T, Yamaguchi H, et al. Structure of the Tfb1/p53 complex: insights into the interaction between the p62/Tfb1 subunit of TFIIF and the activation domain of p53. *Mol Cell* 2006;22:731–40.
31. Strebovsky J, Walker P, Lang R, Dalpke AH. Suppressor of cytokine signaling 1 (SOCS1) limits NFkappaB signaling by decreasing p65 stability within the cell nucleus. *FASEB J* 2011;25:863–74.
32. Saint-Germain E, Mignacca L, Vernier M, Bobbala D, Ilangumaran S, Ferbeyre G. SOCS1 regulates senescence and ferroptosis by modulating the expression of p53 target genes. *Aging* 2017;9:2137–62.
33. De Sepulveda P, Okkenhaug K, Rose JL, Hawley RG, Dubreuil P, Rottapel R. Socs1 binds to multiple signalling proteins and suppresses steel factor-dependent proliferation. *EMBO J* 1999;18:904–15.
34. Giordanetto F, Kroemer RT. A three-dimensional model of Suppressor Of Cytokine Signalling 1 (SOCS-1). *Protein Eng* 2003;16:115–24.
35. Narazaki M, Fujimoto M, Matsumoto T, Morita Y, Saito H, Kajita T, et al. Three distinct domains of SSI-1/SOCS-1/JAB protein are required for its suppression of interleukin 6 signaling. *Proc Natl Acad Sci U S A* 1998;95:13130–4.
36. Yasukawa H, Misawa H, Sakamoto H, Masuhara M, Sasaki A, Wakioka T, et al. The JAK-binding protein JAB inhibits Janus tyrosine kinase activity through binding in the activation loop. *EMBO J* 1999;18:1309–20.
37. Hildebrand DG, Lehle S, Borst A, Haferkamp S, Essmann F, Schulze-Osthoff K. alpha-Fucosidase as a novel convenient biomarker for cellular senescence. *Cell Cycle* 2013;12:1922–7.
38. Kortlever RM, Higgins PJ, Bernards R. Plasminogen activator inhibitor-1 is a critical downstream target of p53 in the induction of replicative senescence. *Nat Cell Biol* 2006;8:877–84.
39. Dos Santos C, McDonald T, Ho YW, Liu H, Lin A, Forman SJ, et al. The Src and c-Kit kinase inhibitor dasatinib enhances p53-mediated targeting of human acute myeloid leukemia stem cells by chemotherapeutic agents. *Blood* 2013;122:1900–13.
40. Lambert JM, Gorzov P, Veprintsev DB, Soderqvist M, Segerback D, Bergman J, et al. PRIMA-1 reactivates mutant p53 by covalent binding to the core domain. *Cancer Cell* 2009;15:376–88.
41. Sherr CJ, Beach D, Shapiro GI. Targeting CDK4 and CDK6: from discovery to therapy. *Cancer Discov* 2016;6:353–67.
42. Kim LC, Song L, Haura EB. Src kinases as therapeutic targets for cancer. *Nat Rev Clin Oncol* 2009;6:587–95.
43. Kong X, Feng D, Wang H, Hong F, Bertola A, Wang FS, et al. Interleukin-22 induces hepatic stellate cell senescence and restricts liver fibrosis in mice. *Hepatology* 2012;56:1150–9.
44. Babon JJ, McManus EJ, Yao S, DeSouza DP, Mielke LA, Sprigg NS, et al. The structure of SOCS3 reveals the basis of the extended SH2 domain function and identifies an unstructured insertion that regulates stability. *Mol Cell* 2006;22:205–16.
45. Qiu X, Guo G, Chen K, Kashiwada M, Druker BJ, Rothman PB, et al. A requirement for SOCS-1 and SOCS-3 phosphorylation in Bcr-Abl-induced tumorigenesis. *Neoplasia* 2012;14:547–58.
46. Huang Y, Wang J, Cao F, Jiang H, Li A, Li J, et al. SHP2 associates with nuclear localization of STAT3: significance in progression and prognosis of colorectal cancer. *Sci Rep* 2017;7:17597.
47. Ke J, Chelvarajan RL, Sindhava V, Robertson DA, Lekakis L, Jennings CD, et al. Anomalous constitutive Src kinase activity promotes B lymphoma survival and growth. *Mol Cancer* 2009;8:132.

Cancer Research

The Journal of Cancer Research (1916–1930) | The American Journal of Cancer (1931–1940)

Phosphorylation of SOCS1 Inhibits the SOCS1–p53 Tumor Suppressor Axis

Emmanuelle Saint-Germain, Lian Mignacca, Geneviève Huot, et al.

Cancer Res 2019;79:3306-3319. Published OnlineFirst May 17, 2019.

Updated version Access the most recent version of this article at:
doi:[10.1158/0008-5472.CAN-18-1503](https://doi.org/10.1158/0008-5472.CAN-18-1503)

Supplementary Material Access the most recent supplemental material at:
<http://cancerres.aacrjournals.org/content/suppl/2019/05/17/0008-5472.CAN-18-1503.DC1>

Cited articles This article cites 47 articles, 13 of which you can access for free at:
<http://cancerres.aacrjournals.org/content/79/13/3306.full#ref-list-1>

E-mail alerts [Sign up to receive free email-alerts](#) related to this article or journal.

Reprints and Subscriptions To order reprints of this article or to subscribe to the journal, contact the AACR Publications Department at pubs@aacr.org.

Permissions To request permission to re-use all or part of this article, use this link
<http://cancerres.aacrjournals.org/content/79/13/3306>.
Click on "Request Permissions" which will take you to the Copyright Clearance Center's (CCC) Rightslink site.